Hydrogeochemical Modelling for Groundwater in Neyveli Aquifer, Tamil Nadu, India, Using PHREEQC: A Case Study

S. Chidambaram,[1] P. Anandhan,[1] M. V. Prasanna,[2,6] AL. Ramanathan,[3] K. Srinivasamoorthy,[4] and G. Senthil Kumar[5]

Sophisticated geochemical models have been used to describe and predict the chemical behaviour of complex natural waters and also to protect the groundwater resources from future contamination. One such model is used to study the hydrogeochemical complexity in a mine area. Extraction of groundwater from the coastal aquifer has been in progress for decades to mine lignite in Neyveli. This extraction has developed a cone of depression around the mine site. This cone of depression is well established by the geochemical nature of groundwater in the region. 42 groundwater samples were collected in a definite pattern and they were analysed for major cations, anions and trace elements. The saturation index (SI) of the groundwater for carbonate, sulphate and silica minerals was studied and it has been correlated with the recharge and the discharge regions. The SI of alumino silicates has been used to decipher the stage of weathering. The $SI_{Gibbsite} - SI_{K\text{-feldspar}}$ has been spatially distributed and the regions of discharge and recharge were identified. Then two flow paths A1 and A2 were identified and inverse modelling using PHREEQC were carried out to delineate the geochemical process that has taken place from recharge to discharge. The initial and final solutions in both the flow paths were correlated with the thermodynamic silicate stability diagrams of groundwater and it was found that the state of thermodynamic stability of the end solutions along the flow path were approaching similar states of equilibrium at the discharge.

KEY WORDS: Hydrogeochemistry, saturation index, inverse modelling, silicate stability, Neyveli aquifer.

INTRODUCTION

Hydrogeochemical composition of groundwater can also be indicative of its origin and history of passage through underground materials which water has been in contact with, in shallow and deep-seated conditions. Natural and anthropogenic sources along with chemical and biogeochemical constituents have been considerably altering groundwater quality in recent years. The computerised geochemical models are powerful tools for understanding the chemical state of natural waters and for predicting the behaviour of such waters under variety of

---
[1]Department of Earth Sciences, Annamalai University, Annamalai Nagar 608002, India.

[2]Department of Applied Geology, School of Engineering and Science, Curtin University, CDT 250, 98009 Miri, Sarawak, Malaysia.

[3]School of Environmental Sciences, Jawaharlal Nehru University, New Delhi, India.

[4]Department of Earth Sciences, School of Physical, Chemical and Applied Sciences, Pondicherry University, Puducherry, India.

[5]Department of Geology, HNB Garwhal University, Srinagar, Uttarakhand, India.

[6]To whom correspondence should be addressed; e-mail: geoprasanna@gmail.com

hypothetical conditions. Helgeson et al. (1970), Plummer et al. (1976), Shannon et al. (1977), Spostigo and Mattigod (1979), Wolery (1979), Felmy et al. (1984), Parkhurst et al. (1990) and many others have developed a variety of geochemical models for describing and deducing the chemical behaviour of complex and mixed waters. A brief review of existing geochemical studies has been given by Nordstrom et al. (1979), Jenne (1981), Plummer et al. (1983), Runnels (1978) and Plummer et al. (1990). Several earlier workers have also used geochemical models for solubility equation study of groundwater (Wolery 1979; Wolery 1983; Tamata 1990; Deutsch 1997; Elangovan 1997; Murphy and Schramke 1998).

The global problems approaches and priorities of chemical modelling were discussed in detail by Jenne (1981). The implication of computer programme in calculation of equilibrium distribution of inorganic species of major and minor elements in natural waters using chemical analysis and in situ measurements of EC, pH were discussed in detail by Truesdell and Jones (1973). Simulation of calcite dissolution and porosity changes in saltwater mixing zone in coastal aquifers was done by Sanford and Konikow (1989). They found that there is an increasing porosity and permeability by enhanced dissolution, using geochemical model PHREEQE. The same model was used by Elangovan et al. (1999) to find out the disequilibrium indices of calcite along with other minerals such as calcite, aragonite, dolomite, hematite, goethite, $Fe(OH)_3$ and strontionite.

The geochemical reaction simulation model WATQ4F (Truesdell and Jones 1973; Plummer et al. 1976) has been used to determine the solubility of equilibria for the groundwater of Gadilam river basin (Prasanna et al. 2006). During the reaction simulation, WATEQ4F calculates the total concentration of elements, log (ratio) for stability plots and distribution of aqueous species, the amount of minerals (or other phases) transferred in or out of the aqueous phase with respect to specified mineral phases. The data required for input to the model include the concentration of dissolved constituents, temperature and pH. The aqueous speciation is computed by an iterative process using equilibrium constant based on the free energy of reaction (Gibbs 1970). Either Davis or extended Debye Huckel equation can be used for the calculation of activity coefficients (Garrels and Christ 1965; Drever 1988). Inverse modelling using PHREEQC was also attempted by Anandhan (2005) and Uma Maheswaran

(2007) for delineating the geochemical process from the recharge to discharge. The value of ionic activity product (IAP) for a mineral equilibrium reaction in natural water may be compared with the value of KT, the solubility product of the mineral. If the value of log IAP is equal to greater than log KT, the natural water is saturated or supersaturated with respect to the mineral. If IAP is less than KT, the solution is undersaturated with respect to the mineral,

Now, this indices log(IAP/KT) was calculated to know if:

SI = log IAP/K = 0; equilibrium state,
SI = log IAP/K < 0; under saturation state (mineral dissolution condition),
SI = log IAP/K > 0; over saturation state (mineral precipitation condition).

In this present study, two specific flow paths have been selected to study the hydrogeochemical variations. XRD analysis of the sediment samples have been used to substantiate the hydrogeochemical model and to incorporate complexity of all relevant geochemical processes. Hence an effort has been made to predict the chemical behaviour of groundwater by processing the data using the hydrogeochemical model PHREEQC.

Study Area

The area chosen for study is Neyveli and adjoining region, which is located in Cuddalore district of Tamil Nadu State, Southern India. The area is bounded between north latitudes 11°40′ and 11°25′ and east longitudes 79°20′ and 79°40′ (Fig. 1). It falls in survey of India toposheets 58 M/6, M/7, M/10 and M/11, with a total area of about 835 km^2. There are two lignite mines in the study area, 1st (14 km^2) and 2nd (26 km^2), which extend from South of Neyveli Township to North of Vellar river. The first mine was started in 1957 and later the second in 1981. The lignite rank of coal with a deposit of about 3,300 million tonnes of reserves is estimated in Neyveli region of Tamil Nadu. To excavate the reserves, very large quantities of groundwater is pumped from underlying aquifer so as to keep piezometric water level below lignite seam. During this, pumping water is extracted from the confined and unconfined aquifers of the Cuddalore formation. Extraction of groundwater due to mining of lignite in both mines is of order of 167.92
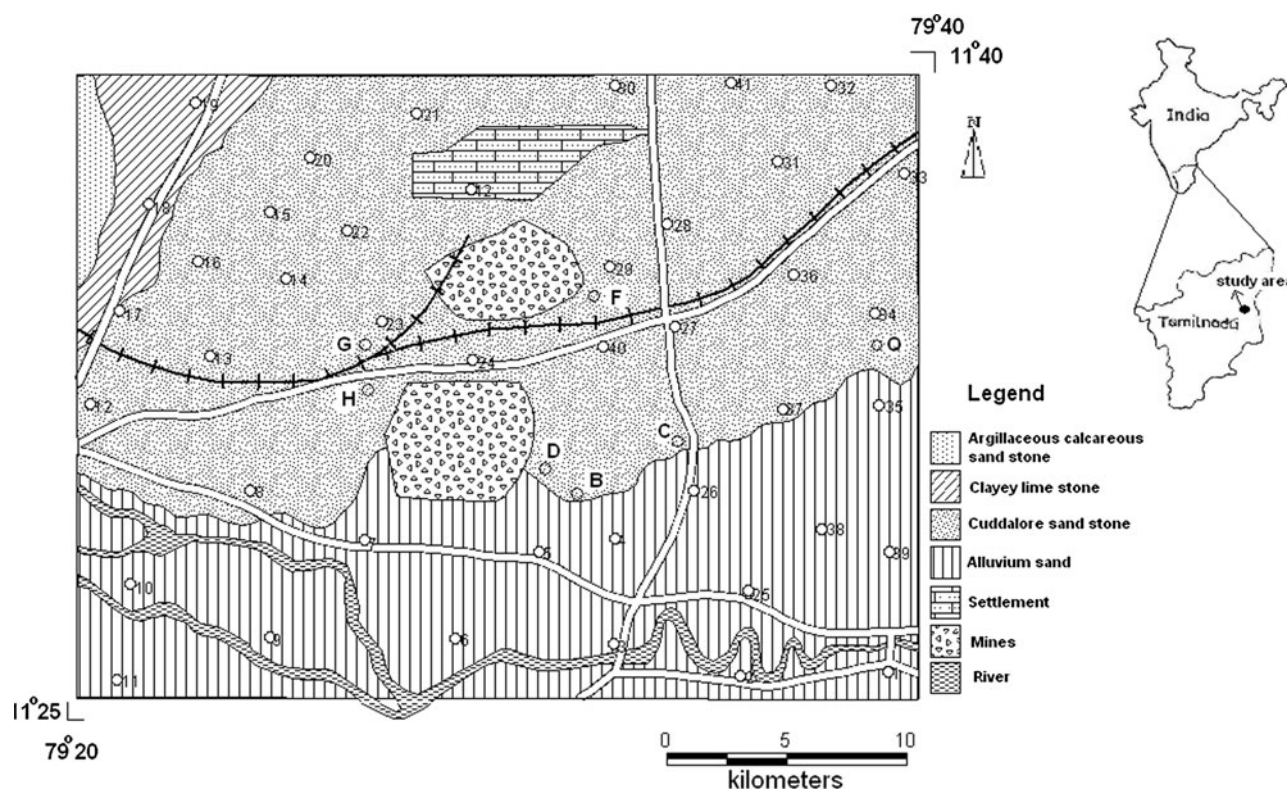
Figure 1. Location and geology of the study area.

Million Cubic Metre (MCM)/year. The cone of depression is formed around the mine site and water from many directions flows towards the depression. The main physiography of study area is flat on eastern side and with high ground in north western portion of 100 m above mean sea level (AMSL). Minimum elevation of the region is below 20 m AMSL. The rainfall received during the northeast monsoon is more effective and contributing 53% of annual precipitation and it ranges between 1000 and 1200 mm.

Geology

Older Archaean formation followed by fossiliferous siliceous limestone, calcareous sandstone and marl exposed as narrow belt is classified under Ariyalur stage of Cretaceous system located in NW and WNW region and strikes NNE–SSW. Ariyalur formation is followed by a succession of black clays or shale, siliceous limestone, calcareous sandstone and shale constituting the Cuddalore series. These rocks are currently believed to be of upper

Mio-Pliocene. It is exposed in almost 65–70% of the study area. Above the Cuddalore sandstone, alluvium occurs as patches derived from Vellar and Manimukthanadhi rivers. The Cuddalore series comprises of argillaceous sandstone, pebble bearing sandstone, ferruginous sandstone, grits and clay beds. The lignite is found in the sandstone of Cuddalore (Gowrishanker et al. 1980). In argillaceous formation, the sandstone is composed of quartz and feldspar ranges in grain size from very fine to coarse. Fire clay and white clay of economic importance are encountered at varying depths depending upon elevation of ground.

Recent deposits contain sediment of fluvial origin. Various types of soil of this region include laterites, lateritic gravel and river alluvium. These fluvial sediments occupy flood plains of Manimukthanadhi and Vellar rivers. Vellar alluvium is of 35 m thickness at Virudhachallam and 40 m around Sethiyathope. Laterites and lateritic gravel, overlies Cuddalore formation. Laterites are generally ferruginous and it occurs fairly extensive in region from Vadalur to east of Neyveli. Laterites are yellow and dark brown in colour with hard nature in

some places. A varied rock types exist in the study area from Archaean basement to recent alluvium and all these formations act as aquifers. The study is restricted to samples from the Cuddalore sandstone aquifer.

Hydrogeology

The shallow aquifers occurring within 35 m BGL (Below Ground Level), generally comprise a mixture of sands, clay, laterites, lateritic sandstones, clayey mottled ferruginous sandstone. The thickness of the aquifers varies from 11 to 70 m. In the study area during pre-monsoon, the depth to water table is in range of 5–20 m, whereas during post-monsoon it rises between 2 and 10 m (Fig. 2). Deep aquifers are composed of fine to very coarse grained sands, pebble and gravels. The depth to water table lies between 30 and 70 m from ground level. It is also noted that the deeper water table is noted around the mine area.

The water table fluctuation ranges between 0.4 and 8.4 m. The minimum level has been recorded in Southern part of the study area and maximum has been recorded at Northwest part of study area. A number of yield tests were also conducted on open well to determine the aquifer parameters like specific capacity, transmissivity, permeability and specific yield (CGWB 1992). The yield of dug wells ranges between 250 and 400 litre per minute (lpm) for a drawdown ranging between 0.5 m to 2.0 m. The specific yield values of shallow aquifer zones ranges between 1.3 and 7%. The range of transmissivity in the study area varies from 167.5 to

544.5 m^2/day. The specific capacity ranges from 122 to 305 lpm/m of draw down.

METHODOLOGY

Forty-two groundwater samples were collected in the study area (Fig. 1). Samples were collected from the Cuddalore sandstone aquifer. Water samples were analysed for major, minor and trace ion concentration by using standard procedures (APHA 1995; Ramanathan 1992; Ramesh and Anbu 1996). The samples were collected from depths ranging from shallow aquifers. The collected samples were analysed for the major cations like Ca and Mg (titrimetry), Na and K (Flame photometer CL 378); anions, Cl and HCO_3 (titrimetry), SO_4, PO_4, and H_4SiO_4 by spectrophotometry (SL 171 minispec). The EC and pH were determined in the field using electrodes.

Analyses of the heavy metals were done, after the samples were filtered through 0.45-μm membrane filter paper using vacuum pumps. The samples were then spiked with the standard solution of the metals chosen for analysis. This standard addition method was adopted to achieve greater accuracy in the analysis of trace metals such as Fe, Mn, Cu, Co, Zn, Cr, Pb and Al.

Sediment cores were collected in upper 1 m in selected locations and used to study the secondary minerals present. 9 samples were collected for X-ray diffraction analysis around the mining area (Table 1). The size fractions were separated and slides were prepared and analysed for the presence of secondary minerals. The mineralogy of sediments was also studied by X-ray diffraction. The slides were prepared by drop on slide technique. The samples were run on Philips X-ray diffractometer using Cu and Kα ration source and Ni filter. The chart drive/cm/min, goniometer 1°/min and intensity of 2×10^2 were maintained.

RESULTS

The chemical composition of the groundwater samples of the study is given in Table 2. Groundwater is generally alkaline in nature with pH ranging from 5.78 to 7.9 with an average of 7.11. EC ranges from 178 to 2970 μS/cm with an average of 795 μS/cm. Total dissolved solids (TDS) which is generally the sum of dissolved ionic concentration
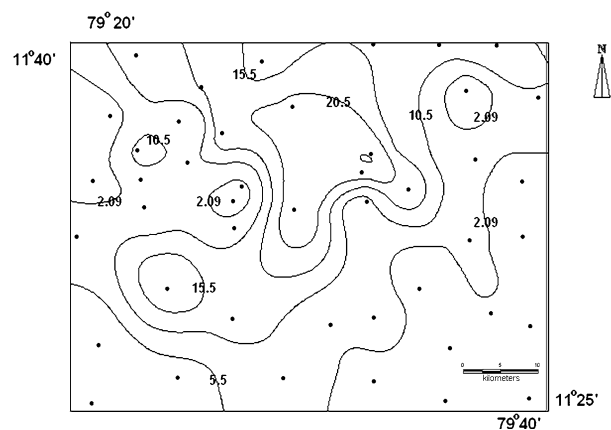
Figure 2. Water level contour map in the study area (in metres below ground level).

Table 1. Result of the XRD analysis of the sediment samples

Location	Marcasite%	Quartz%	Kaolinite%	Gypsum%	K-Feldspar%	Anhydride%	Chlorite%
Periyakurichi	0	61.1	29.5	0	0	0	0
Melkuppam	0	30.5	0	64.1	5.41	0	0
Karaimedu	0	72.8	23.6	0	0	0	0.6
Karuvetti	0	69	30.9	0	0	0	0
Veenankeni	0	54.3	0.6	0	42.2	2.9	0.4
Near Mine II	3.99	6.9	12.3	0	83.5	0	0.8
Mudanai	0	25.5	4.8	0	0	0	0
Merkiruppu	0	34.6	0	0	0	0	0
Vadakuvelur	0	47.5	15.5	0	0	0	0
Near I Mine	3.5	67.1	2.5	22.1	19.5	0	0.9

Table 2. Chemical Composition of Groundwater (all Values in ppm Except pH and EC in µS/cm)

S. no.	pH	EC	Cl	CO_3	HCO_3	SO_4	PO_4	NO_3	F	H_4SiO_4	Ca	Mg	Na	K	TDS
1	7.95	2120	345.64	60	329.4	610	1.75	5	1.5	30	6	13.2	936	23	2205.73
2	7.65	1780	319.05	18	225.7	412	0.15	3	0.2	29	12	13.2	420	8	1362.82
3	8.32	685	93.49	18	146.4	109	0.15	2.15	0.19	7.9	12	3.59	180	2	509.11
4	7.8	2490	487.44	12	176.9	495	0.25	3	0.19	24	24	15.6	680	3	1845.82
5	7.92	2060	363.36	12	231.8	398	0.03	3.35	0.5	28	20	20	270	10	1259.52
6	7.72	1110	177.25	12	176.9	342	0.15	2	0.23	30	27	15.6	168	8	883.57
7	7.5	1530	274.74	18	97.6	321	0.7	1.85	0.25	27.75	15	16	320	11	1057.65
8	7.93	836	88.63	12	195.2	142	0.15	2	0.2	25.4	12	12	240	8	654.7
9	8.25	1110	159.53	18	213.5	241	0.2	0.5	0.06	14.4	10	15.6	425	12	1017.19
10	7.64	930	141.8	24	176.9	320	0.25	2.4	0.57	28	18	7.2	310	16	964.76
11	8.25	403	17.72	6	122	98	0.15	2.5	0.24	17	14	4.8	44	10	285.21
12	8.35	363	26.59	18	85.4	79	0.09	2.5	0.52	26.5	14	1	49	3	263.24
13	8.25	295	26.59	18	103.7	17	0.13	3	0.17	20	12	3.6	30	6	191.51
14	8.3	245	26.59	12	85.4	15	0.14	0.5	0.18	9	12	1.2	20	3	146.05
15	8.17	391	35.45	18	134.2	78	0.12	2	0.23	12	20	1	82	11	332.12
16	8.2	500	44.31	0	103.7	110	0.07	1.5	0.18	30	10	4.8	95	12	370.08
17	7.68	1030	97.49	18	244	304	1.55	3.2	0.24	23	20	3.6	318	6	934.28
18	7.89	1250	150.66	12	176.9	328	0.4	3.2	0.59	30	15	19.2	258	10	928.39
19	8.45	448	124.08	6	79.3	110	0.3	3.2	0.18	18.3	20	1.2	49	9	386.44
20	8.21	220	17.73	18	73.2	96	1.45	2.2	0.12	30	4	4.8	20	5	236.02
21	8.52	163	8.86	6	73.2	75	1.3	1.1	0.08	10	10	1	3	2	158.86
22	8.21	183	17.73	18	79.29	15	1.8	2.2	0.05	30	8	1.2	17	3	154.36
23	8.6	545	79.76	6	79.3	120	1.55	2	0.06	13.5	20	2.4	88	5	383.45
24	8.11	6621	88.63	12	97.6	478	0.15	1.5	0.07	28	20	2.4	135	4	823.51
25	7.85	1580	230.43	42	347.69	340	0.1	3	0.8	25	22	1.2	690	10	1556.344
26	8.05	1740	257.01	36	213.5	110	0.1	2.5	0.08	27	20	4.8	750	6	1327.19
27	8.25	546	88.63	6	67.1	97	0.6	3.7	0.12	30	18	1.2	14	3	300.11
28	8.15	399	70.9	12	109.79	71	0.1	2.3	0.11	29	10	19.2	55	27	357.684
29	8.05	245	26.59	18	71.2	48	0.1	2.5	0.2	25.5	14	2.4	30	3	205.81
30	6.98	155	44.31	0	67.7	18	0.15	0.5	0.35	28	8	2	22	2	165.93
31	6.92	327	35.45	12	97.6	21	0.15	2.6	0.24	7.3	17	1	38	6	193.5
32	7.9	197	17.73	12	67.1	18	0.2	2	0.32	19.05	12	1	21	1	138.76
33	7.23	431	26.59	12	128.1	27	0.1	2.35	0.2	26	16	3.6	67	3	255.9
34	8.26	776	194.98	12	91.5	79	0.5	2.1	0.26	12	30	1	142	12	534.94
35	8.65	1760	265.88	18	183	189	0.2	2.5	0.18	1.6	20	6	400	18	1023.96
36	7.25	1000	239.29	12	91.5	247	0.95	3.7	0.18	26	23	8	272	15	897.22
37	7.53	1040	212.7	0	178.89	231	1.45	2	0.5	21	28	7.2	220	25	856.18
38	7.68	900	115.21	18	146.4	192	0.1	1.85	0.27	27	17	1.2	230	38	721.27
39	7.58	1220	274.74	12	146.4	181	0.95	1.85	0.18	28	26	10.8	527	26	1171.56
40	8.21	670	106.35	18	115.9	142	0.5	1.15	0.25	13	18	4.8	185	10	561.39
41	8.5	271	26.59	12	85.4	52	0.15	2.1	0.12	28	10	3.6	28	4	213
42	8.1	193	26.59	12	67.9	17	0.25	2.4	0.12	26	14	1.2	14	2	151.5

Table 3. Concentration of Heavy Metals in the Study Area (all Values in ppm)

S. no.	Location	Cu	Mn	Fe	Cr	Zn	Co	Pb	Al
1	Bhuvanagiri	0.96	0.56	1.23	0.54	0.55	0.51	0.03	1.80
2	Orathur	0.89	0.48	2.05	0.28	0.44	0.42	0.02	2.00
3	Sethiathope	0.85	0.79	1.36	0.64	0.58	0.27	0.02	1.70
4	Thurungikollai	1.12	0.88	1.24	0.22	0.48	0.65	0.03	2.30
5	Valayamathevi	0.99	0.97	1.22	0.41	0.36	0.44	0.03	1.70
6	Agaramalambadi	0.68	0.68	2.21	0.32	0.55	0.52	0.03	2.11
7	Kammapuram	0.78	0.56	2.24	0.14	0.29	0.44	0.04	1.25
8	Gopalapuram	0.89	0.70	1.65	0.36	0.41	0.46	0.03	1.83
9	Kavanur	0.46	0.78	1.35	0.28	0.47	0.42	0.02	2.01
10	Karmangudi	0.85	0.48	1.59	0.19	0.41	0.36	0.03	1.70
11	Rajendrapatinam	0.69	0.55	1.96	0.15	0.26	0.41	0.04	1.85
12	Annanagar	0.75	0.87	1.88	0.32	0.42	0.44	0.03	2.21
13	Erupukurichi	1.14	0.69	2.08	0.24	0.25	0.42	0.03	1.90
14	Mudanai	1.25	0.55	2.16	0.35	0.26	0.43	0.04	2.20
15	V.Reddikuppam	0.86	0.65	1.84	0.26	0.35	0.41	0.03	1.98
16	Kotteri	1.04	0.69	3.15	0.42	0.53	0.41	0.03	1.85
17	Irusalakuppam	0.99	0.49	1.85	0.32	0.42	0.36	0.03	1.75
18	Viredykuppam	1.02	0.59	2.50	0.37	0.48	0.39	0.03	1.80
19	Irusalakurichi	0.65	0.85	2.36	0.33	0.55	0.37	0.02	2.15
20	Merkirupu	0.87	0.79	1.59	0.22	0.29	0.36	0.05	2.10
21	Kattukoodalur	0.89	0.85	2.24	0.25	0.36	0.29	0.02	1.75
22	Chinnakappankulam	0.58	0.99	2.85	0.24	0.43	0.27	0.03	1.90
23	Kunnankurichi	0.79	0.61	2.64	0.32	0.26	0.26	0.03	1.80
24	Mandarakuppam	0.84	0.78	2.75	0.33	0.44	0.24	0.02	2.20
25	Odayur	0.77	0.81	2.41	0.28	0.39	0.30	0.03	1.98
26	Karaimedu	0.72	0.68	0.99	0.26	0.26	0.27	0.02	1.70
27	Vadalur	0.69	0.39	2.22	0.24	0.37	0.38	0.01	2.30
28	Vadakuthu	0.85	0.69	1.99	0.31	0.40	0.39	0.03	1.92
29	Vadakumelur	0.79	0.73	2.23	0.29	0.38	0.32	0.03	1.96
30	Marungur	0.76	0.66	1.97	0.27	0.36	0.33	0.02	1.97
31	Vengadampettai	0.88	0.86	3.25	0.31	0.31	0.37	0.04	1.80
32	Pudukuppam	0.76	0.89	3.64	0.32	0.28	0.42	0.03	2.10
33	Navakulam	0.82	0.88	3.45	0.32	0.30	0.40	0.04	1.95
34	Kannadi	0.86	0.74	3.54	0.35	0.24	0.26	0.34	2.20
35	Kothavacheri	0.87	0.79	2.89	0.26	0.37	0.37	0.05	1.90
36	Kurinjipadi	0.87	0.77	3.22	0.31	0.31	0.32	0.19	2.05
37	Kalkunam	0.69	0.88	2.26	0.28	0.28	0.29	0.04	1.81
38	Krishnapuram	0.81	0.82	3.17	0.31	0.30	0.34	0.12	2.00
39	Melmanakudi	0.78	0.68	2.64	0.27	0.26	0.48	0.03	2.10
40	Seplanatham	0.79	0.59	3.06	0.22	0.52	0.47	0.03	1.27
41	Manadikupam	0.59	0.81	2.89	0.21	0.36	0.52	0.04	1.70
42	Neyveli	0.88	2.39	0.20	0.38	0.37	0.04	1.51	0.81

varies between 125.55 and 1313.9 mg/l with an average of 554.17 mg/l. The results of heavy metals concentration of the region are given in Table 3.

Anions

Anion chemistry shows chloride is most abundant ion in most locations and in some place it is equal to sulphate. Cl^- and SO_4^{2-} are followed by HCO_3^-, NO_3^-, PO_4^- and F^-. Chloride concentration in samples varies between 8 and 458 mg/l with

an average of 141.02 mg/l. Bicarbonate concentration varies between 12.2 and 384.2 mg/l with an average of 123.49 mg/l. Carbonate varies between below deduction limit (BDL) to 24 mg/l with an average of 5.14 mg/l. Fluoride ranges from 0.01 to 0.72 mg/l with average value of 0.15 mg/l.

Sulphate ranges from 0.01 to 368 mg/l with an average of 114.79 mg/l. Sulphate is usually derived from oxidative weathering of sulphide bearing minerals like marcasite. The presence of marcasite in the mines indicates that the lignite is deposited in the reducing environment. Higher concentration of

sulphate in the study area could be due potential additional sources like clay and lignite beds, besides oxidative weathering of marcasite in this region.

The order of dominance of minor ions is $H_4SiO_4 > NO_3^- > PO_4^{2-}$. Silica ranges from 8 to 147.5 mg/l with an average of 35.98 mg/l. Existence of alkaline environment and abundance of silicate minerals in the study area enhance solubility of silica, in turn their concentration in groundwater. Nitrate ranges from 0.01 to 6 mg/l with an average of 2.12 mg/l. Nitrate content is well within the permissible limit. Phosphate ranges from 0.01 to 8.8 mg/l with an average of 2.08 mg/l.

Cations

Dominance of cations in the study area is as follows: Na > Ca > Mg > K. Na ranges from 22 to 365 mg/l, with an average of 147.17 mg/l. Ca ranges from 3 to 42 mg/l with an average of 16.57 mg/l. Magnesium concentration ranges from 1 to 52 mg/l with an average of 9.46 mg/l. Potassium ranges from 1 to 43 mg/l with an average of 8.38 mg/l. Potassium is lesser than sodium due to its greater resistance to weathering and formation of clay minerals. Because of its low solubility, its concentration is much lower than Na.

DISCUSSION

PHREEQC determines the saturation index (SI) of different minerals in various solutions and mixtures. A positive SI indicates super saturation or precipitation of secondary minerals and a negative SI indicates the under saturation or dissolution of minerals. An SI of ±0.5 indicates equilibrium conditions.

Saturation Index of Groundwater for the Chief Minerals

Carbonates

The change in pH of water results in precipitation of CaCO$_3$ as dissolution of carbonate minerals takes place when there is a variation in pH and HCO$_3$. In a closed system dissolution process, carbonic acid is consumed and not replenished from
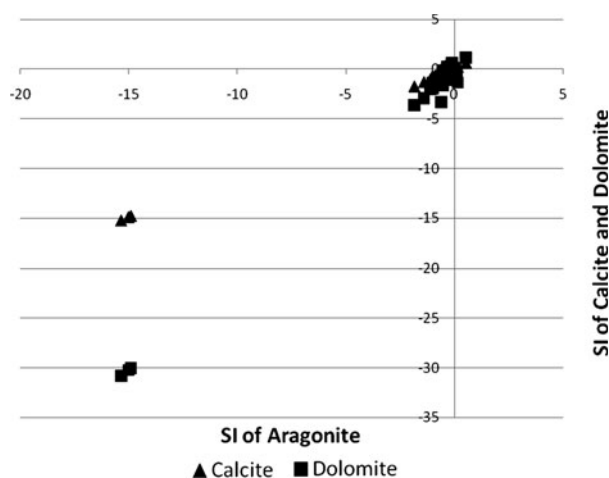

Figure 3. Saturation index of carbonate minerals.

outside the system as dissolution proceeds. SI of ground water for the carbonate minerals (Fig. 3), aragonite, calcite and dolomite, were calculated. Figure 3 represents the relationship between the SI of aragonite (x-axis) and SI of calcite and dolomite (y-axis). It is noted that the carbonate SI are under-saturated or near saturation with respect to all the minerals. These differentiations in the SI of the carbonate mineral may also useful in identifying the recharge and discharge zones. Figure 3 shows that SI of samples 22, 23 and 24 are highly under-saturated with respect to calcite, dolomite and aragonite. Though this SI for these minerals are negative, they are in the following order: Dolomite < Aragonite < Calcite.

Silica

When saturated the dissolved silica may attain a crystalline (quartz: QTZ), cryptocrystalline (Chalcedony: CHAL) or amorphous form (SiO$_2$ (a)). The SI of groundwater of the region (Fig. 4) reveals that the amorphous form is always under-saturated and it is saturated with the crystalline form. The cryptocrystalline form is just saturated and the index of saturation for this water fluctuates from under saturation to near saturation in few locations. SI of quartz minerals like chalcedony, quartz and amorphous silica indicates that SI_{QTZ} in all the samples is saturated. The SI of the silica minerals is in the following order: $SI_{QTZ} > SI_{CHAL} > SI_{SiO_2 (a)}$ (crystalline > cryptocrystalline > amorphus).

Figure 4. Saturation index of silicate minerals.
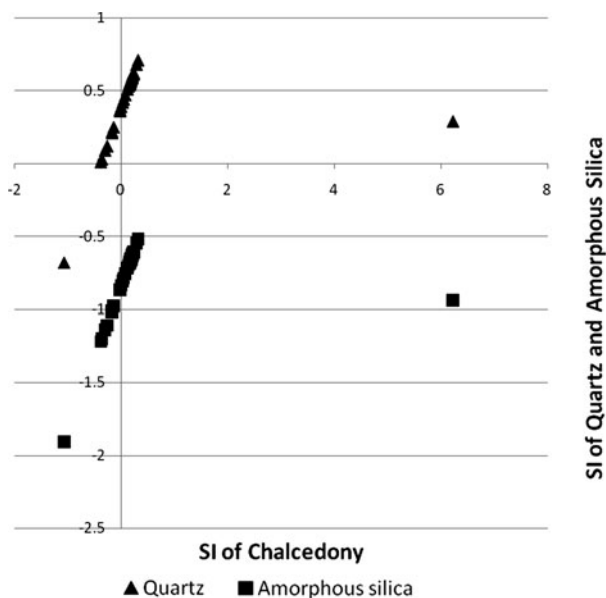

Figure 5. Saturation index of alumino silicates.

A metastable phase should be looked upon as the upper limit of dissolved silica content of natural waters for most low temperature processes. Maximum silica solubility at low temperature is controlled by amorphous silica rather than by quartz. It is clear from this plot that the discharge regions 22, 23 and 24 distinctly as represented in the other plots are not well-defined here.

Alumino Silicates

Most important among the weathering reactions is the congruent dissolution of alumino silicates. The primary mineral is converted to secondary mineral. The structural breakdown of alumino silicates is accompanied by release of cation and usually silicic acid (Stumm and Morgan 1996). As a result of such reactions, alkalinity is imparted to the dissolved phase from the bases of the minerals. In most of the silicate phases, since Al is usually conserved during the reaction the solid residue has a higher Al content than the original silicates. The dissolution of alumino silicates in groundwater is strongly influenced by the chemically aggressive nature of water. The SI of secondary minerals in groundwater (Fig. 5) is in the following order: K-mica > Kaolinite > Ca-montmorillonite > Gibbsite > K-feldspar. More variation is noted in SI for gibbsite than K-feldspar indicating the differential intensities of weathering.

The PHREEQC modelling shows that the most of the secondary minerals are saturated and the carbonates are under-saturated to equilibrium in nature.

Sediment Chemistry

The data indicates the presence of quartz and kaolinite in the region without the influence of mine drainages. The sample points B, C, D, F, G, H and Q were shown in Figure 1. The samples from points H and G have gypsum and K-feldspar in addition to kaolinite and quartz; this might be due to the mixing of effluents from mine I, Thermal and Fly ash pond. The sample F is along the downstream flow path of the mine I effluent shows the presence of quartz, K-feldspar, kaolinite and anhydrite. The upstream samples showed the presence of gypsum which is noted here as anhydrite. D and B show the presence of the kaolinite and quartz as they are located in the influence of second mine drainage. The first and second mine drainage stagnates at C (Walaja tank). It shows the minerals similar to the second mine drain regions, as it is located near the mine II and hence the influence of drain waters from this mine is more than the Mine I in the Walaja tank. The mixture of this drainage then migrates to Perumal Eri. The minerals at this location Q show the presence of marcasite, quartz, feldspar and chlorite.

Weathering of primary minerals in nature, results in the formation of secondary minerals along with discharge of ions into aqueous system. Hence it is inferred that water as a medium plays a significance role in dissolving the primary minerals and leaching of ions and thereby formation of secondary minerals. In general sedimentary terrain is chiefly composed of minerals resistant towards weathering like quartz, feldspars and mica. Analysis of XRD data (Table 1) helps in identifying the resultant secondary minerals formed by weathering of primary minerals. The ions which has entered or removed out of system can be easily identified in this process. The Lithology of the study area is chiefly composed of K-feldspars and quartz. The resultant secondary minerals identified are quartz, kaolinite, gibbsite, gypsum, anhydrite and marcasite. The formation of these minerals is generally favoured by removal of cations like K^+, Na^{2+} and Mg^{2+} (Konrad 1983). Silica is also removed from the system. These ions after attaining freedom from structure enter into aqueous medium. So the composition of water is chiefly charged with these cations apart from anthropogenic influences. Groundwater tends to contain higher concentrations of HCO_3 and other solutes. During the process of weathering, release of bicarbonate is also possible as witnessed by reactions, which may be schematically represented by

$$Cation\,Al\text{-}Silicate + H_2CO_3 + H_2O$$
$$= HCO_3 + H_4SiO_4 + Cation + Al\text{-}Silicate(s)$$
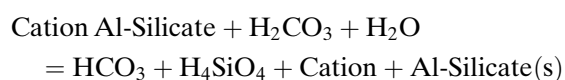
This released ion combines with Mg^{2+} released by weathering of micas results in the formation of secondary carbonates. It is also noted that Cuddalore formation are chiefly composed of marcasite. Sulphide ions from this mineral gets oxidised and migrates as SO_4^{2-}. In the process of transportation it combines with Ca^{2+} present in aqueous medium forms gypsum or anhydrite. Apart from natural process of weathering there is also a possibility of introduction of fertilisers into the system due to the presence of agricultural fields in these regions. This may contribute K^+, Ca^{2+}, Mg^{2+} and SO_4^{2-} ions and also enhance the formation of the sulphate minerals (Anandhan 2005).

Identification of Recharge and Discharge Sites by Saturation Indices

The state of thermodynamic equilibrium between the mineral phase and the water medium helps us to identify the intensity of weathering and the possible directions of the future reaction. This has been made possible by thermodynamic silicate stability diagrams (Garrels and Christ 1965; Drever 1988). Minerals of kaolinite group are the main alteration products of weathering of feldspar. Besides kaolinites, montmorillonites and micas, there are also other possible intermediate products. In the silicate stability diagrams it is understood that at the initial stages when the weathering is initiated the liquid becomes stable with gibbsite, later with kaolinite, and then either with mica or K-feldspar.

In this scenario, the water having positive SI for gibbsite indicates the initial stages of weathering and those with K-feldspar indicates intensive stages of weathering. This intensive stage of weathering is mainly attained by longer residence time of the liquid medium in the rock matrix (Chidambaram 2000). The difference in SI of gibbsite to that of the SI of K-feldspar (SIy = SIg − SIk) helps us to find the region with initial stages of weathering or the zones of recharge and the regions of intensive weathering or the zones of discharge (Fig. 6). Hence the entire study area has been classified into as initial, transitional and final stages of weathering based on SIy values. In the regions with initial stages of weathering SIy is positive and the negative values in the regions coincides with the regions of discharge or the final zones. The near zero values fall in the transitional zones. Hence they can be broadly classed as initial transitional or final stages. The region of recharge are located in NW part of the study area, samples 29 to 36, they are identified as regions with initial state of weathering apart from these samples 3, 4, 14, 15 and 18. Sample numbers 1, 6, 16, 18, 20, 28, 38, 39 and 41 show later stages of reaction and they are in the transition states. Sample numbers 22, 23 and 24 show extreme negative SIy and they are located around mine I it shows the regions of discharge due to the pumping from mines. Thus the regions of recharge and discharge are identified along with their pathways.

Inverse Modelling

Inverse geochemical models quantify net solute flux from water–rock interactions. Geochemical reactions (precipitation/dissolution, redox and surface complextion) between the water and the aquifer material will change the mass of dissolved species, typically in millimol concentrations. Assumptions of
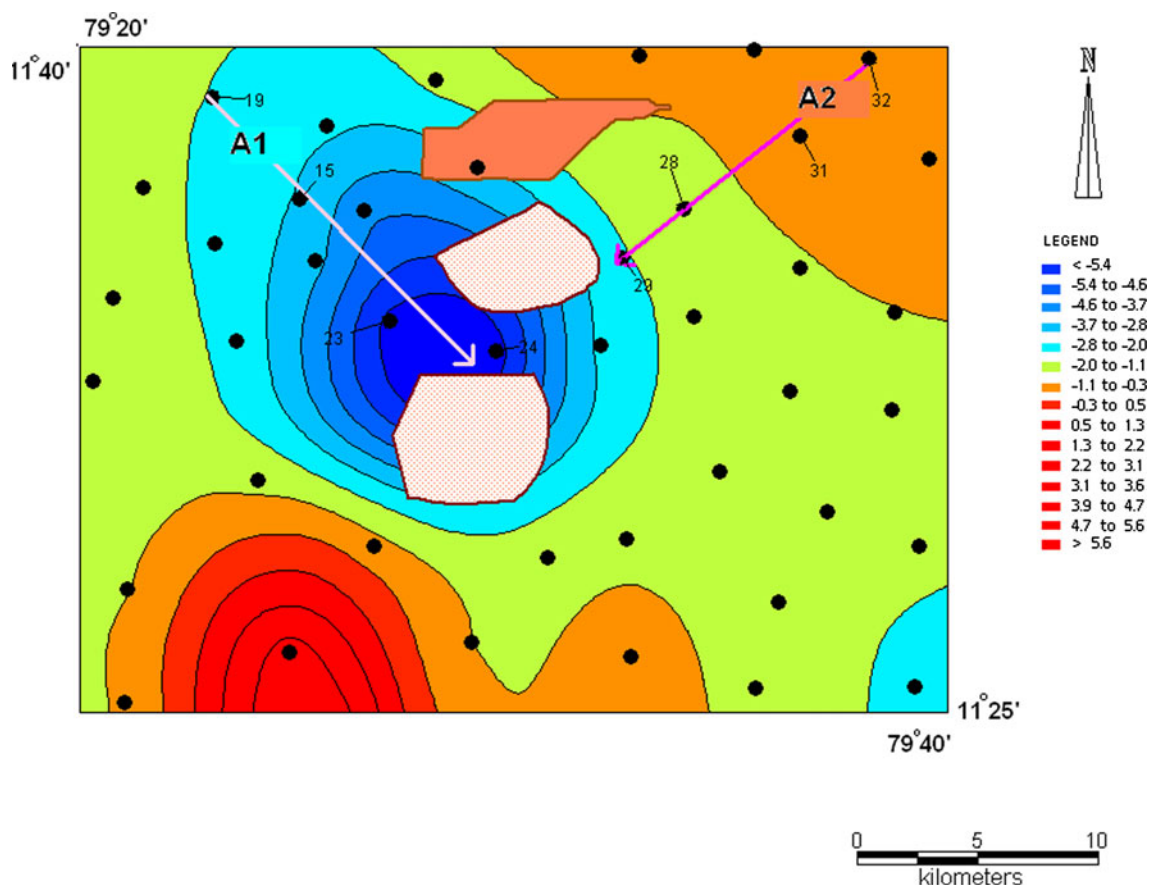
Figure 6. Spatial of SI (gibbsite–K-feldspar).

inverse models are: (1) initial and final conditions occur along the flow path, which are hydraulically connected, (2) dispersion and dissolution do not affect dissolved concentrations, (3) reactions are at steady state, (4) major reactive mineral phases have been identified in the aquifer material (Zhu and Anderson 2002). A model is a subject of the selected phases that satisfies all the selected mass balance constraints. The model is of the form

Initial water + ''Reaction Phases'' →

Final Water + ''Product Phases''.
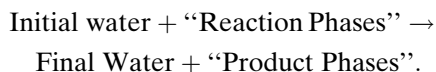
Two prominent pathways A1 and A2 were selected from the identified recharge to discharge.

Flow Path A1

The model inputs are measured initial and final water-quality conditions. The initial condition is represented by water at the recharge region and the final

condition at the discharge region. 'A1' is a pathway extending from the NW of the study area to the mine site; it includes the sample numbers 19 and 24. In this pathway 19 is considered as the initial and 24 as the final solution. For data input to PHREEQC, identifiers in the INVERSE MODELLING data block were used for the selection of aqueous solutions, reactant phases include Ca-montmorillonite, chlorite(14A), gibbsite, kaolinite, K-feldspar, K-mica, marcasite, calcite, aragonite and quartz. The phases were selected after obtaining the XRD patterns from the core samples of the aquifer matrix.

The output of the run has evolved five different types of models giving their respective solution fractions and phase mole transfer. The study of the SI of minerals indicates that there is increase of SI of minerals like Ca-montmorillonite, gibbsite, K-mica, K-feldspar and kaolinite. Precipitation of chlorite and dolomite along its pathway was noted.

The five models are now calibrated to achieve the appropriate field model by establishing the

Table 4. Phase Mole Transfer in Flow Path A1 (All Minerals Mass Transfer is in mill mol kg/l)

	Model I	Model II	Model III	Model IV	Model V
Ca-montmorillonite	−1.276e−003	0.000e+000	0.000e+000	0.000e+000	−6.275e−004
Gibbsite	−1.441e−003	3.888e−003	−1.502e−003	3.909e−003	−2.322e−003
Kaolinite	−1.224e−003	0.000e+000	−1.120e−003	0.000e+000	0.000e+000
Quartz	0.000e+000	2.447e−003	0.000e+000	2.409e−003	0.000e+000
Dolomite	0.000e+000	0.000e+000	−3.487e−003	0.000e+000	−3.488e−004
Chlorite(14A)	7.322e−004	6.912e−004	6.580e−004	7.364e−004	6.787e−004
K-feldspar	0.000e+000	4.027e−003	4.135e−003	0.000e+000	3.827e−003
Marcasite	3.185e−005	0.000e+000	3.642e−005	0.000e+000	−

Table 5. Phase Mole Transfer in Flow Path A2 (All Minerals Mass Transfer is in mill mol kg/l)

	Model I	Model II	Model III	Model IV
Ca-montmorillonite	2.354e−004	5.985e−005	2.983e−005	2.723e−005
Gibbsite	0.000e+000	5.816e−005	−1.174e−003	0.000e+000
Kaolinite	0.000e+000	0.000e+000	0.000e+000	4.878e−005
K-feldspar	−2.017e−004	0.000e+000	3.262e−005	0.000e+000
K-mica	0.000e+000	0.000e+000	0.000e+000	0.000e+000
Marcasite	−	4.461e−005	4.527e−005	4.527e−005

relationships noted in Table 4. The addition and removal are considered as dissolution and precipitation of the phases from the system, respectively. This is derived by the positive and negative symbols respectively, in the phase mole transfer. Hence, dissolution is noted by positive values in phase mole transfer. Thus the alteration product kaolinite and marcasite was noted in two models I and III only. Hence these two models were further calibrated. Model III shows the addition of K-feldspar, marcasite, chlorite and kaolinite, and this is further calibrated with the XRD data of the sediment near the discharge site. So the model III is appropriate field model. It is evident from the model that there has been addition of these compositions in moles along the selected pathway.

Flow Path A2

'A2' is considered as the second pathway, this extends from the NE part of the study area to the mine site it includes sample numbers 32 and 29. In this pathway sample 32 is taken as the initial solution and 29 as the final solution. Data block were used for the selection of aqueous solutions 32 and 29, reactant phases include Ca-montmorillonite, chlorite (14A), gibbsite, kaolinite, K-feldspar, K-mica and quartz (Table 5).

The output of the run has evolved four different types of models giving their respective solution fractions and phase mole transfer. The results of these models were then compared with the XRD data (Table 6). The study of the SI of minerals indicates that there is an increase of SI of minerals like Ca-montmorillonite, K-mica, K-feldspar, aragonite, chlorite and quartz. Precipitation of gibbsite and kaolinite is noted along its pathway.

The process of calibration is done by the identifying the model with the removal of gibbsite and addition of K-feldspar, Ca-montmorillonite and marcasite. This has matched with one model (Model III) and this is adopted as the appropriate field model along its path, where gibbsite and kaolinite is removed from the system and addition phase mole transfer representing progressive weathering of minerals.

Thermodynamic Stability

If the assumption is made that silicate minerals are in equilibrium with pore waters that bathe them, the interrelations of the minerals can be shown as a functions of the activities of the ions dissolved in the water. It is possible to develop qualitative diagrams that are useful to provide a graphic summary of the mineral sequence that might be expected if equilibrium were attained (Garrels and Christ 1965). The stability of the initial and final samples in the flow path A1 shows that there is a small increase of Na and H_4SiO_4 into the system. In Na system the reaction proceeds towards, Na-montmorillonite

which is similar in Ca-montmorillonite (Fig. 7). But in K there is a change in stability field as it shifts from muscovite to kaolinite this might because of the reaction (Fig. 8).

Table 6. SI of Chief Minerals in the Initial and Final Solution in Different Flow Paths

Chief Minerals	Initial	Final
Flow path A1		
Sec.Minerals		
Ca-montmorillonite	4.65	5.13
Chlorite	3.41	1.8
Gibbsite	1.37	2.12
Kaolinite	5.41	6.29
Al-silicate		
K-mica	11.36	11.98
K-feldspar	2	2.22
Carbonate		
Dolomite	−0.44	−0.92
Flow path A2		
Silica		
Quartz	0.45	0.57
Carbonate		
Calcite	−0.38	−0.25
Aragonite	−0.83	−0.39
Al-silicate		
Albite	0.36	0.68
K-feldspar	1.86	0.68
K-mica	11.63	12.16
Sec.Minerals		
Ca-montmorillonite	5.85	6
Chlorite	–	2.49
Gibbsite	2.42	2.27
Kaolinite	6.58	6.52

$$\text{Muscovite} + 2\text{H}^+ + 3\text{H}_2\text{O} \rightarrow 3\text{Kaolinite} + 2\text{K}^+$$
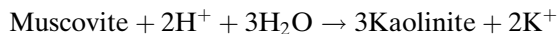
There is a decrease of Ca, Mg and K concentration from the recharge to discharge. This is due to the dilution of Ca and Mg which is present in the initial water. The higher Ca and Mg in this water are attributed to the presence of limestone formation in north western part beyond the study area. In Mg system (Fig. 9) the removal of Mg is noted by the downward migration of the composition in kaolinite field. In general, there is an increase of H_4SiO_4 in the graph. This may help is increasing the SI of Kaolinite and K-feldspars. The stability diagram of Ca system is shown in Figure 10.

Though Ca and Mg are removed from the system but still the reaction proceeds to montmorillonite field by the increase of silica concentration.
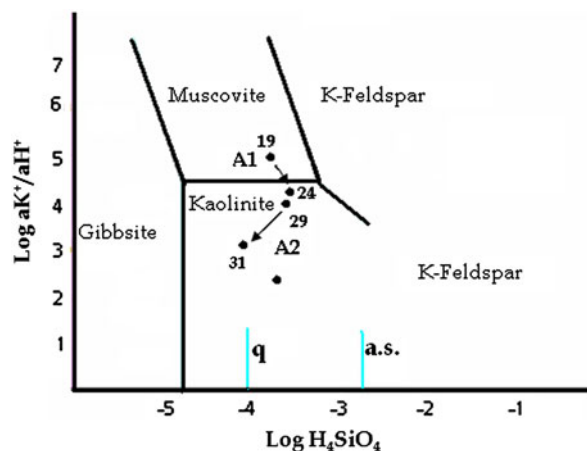

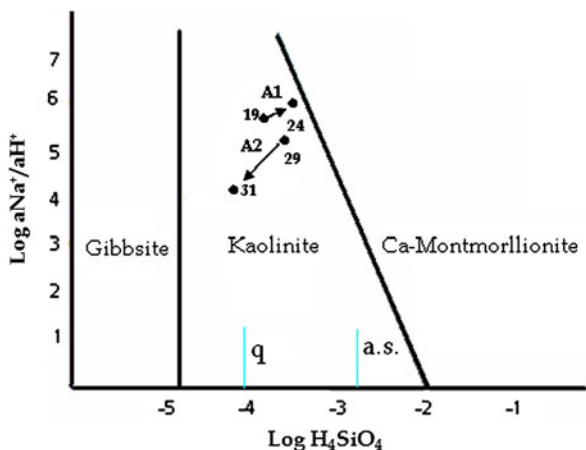**Figure 8.** Thermodynamic stability of samples from recharge and discharge in K system.

Figure 7. Thermodynamic stability of samples from recharge and discharge in Na system.
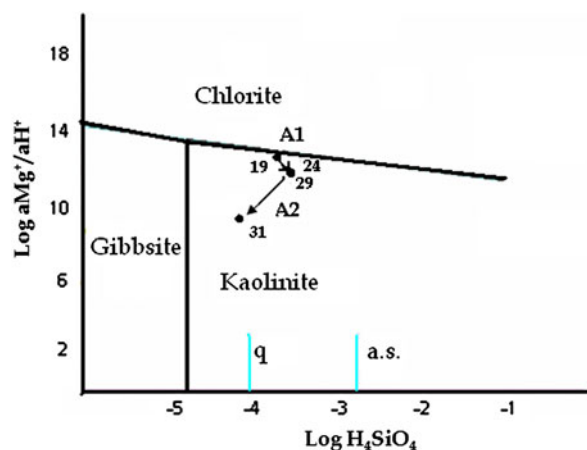

Figure 9. Thermodynamic stability of samples from recharge and discharge in Mg system.
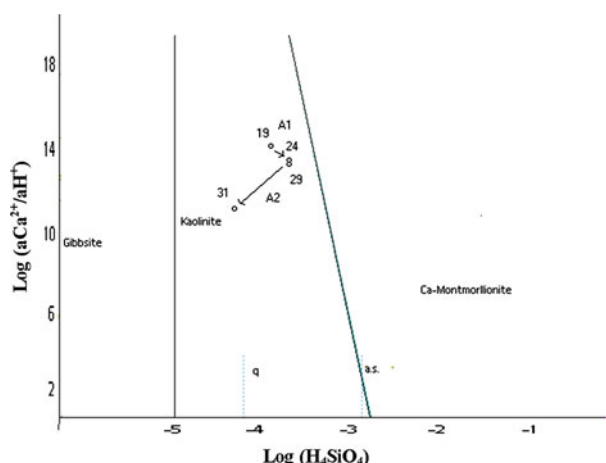
Figure 10. Thermodynamic stability of samples from recharge and discharge in Ca system.

Figure 11. Piper plot for the groundwater of the study area.

In the flow path A2 there is a progressive increase of cation concentration along with silica from the recharge to the discharge. Both, the initial and final composition fall in kaolinite field in all the silicate stability diagrams.

In general the composition of waters from flow paths A1 and A2 marches towards the similar composition at the discharge either by the precipitation of ions or by dissolution.

Groundwater from the recharge regions to the discharge shows difference in composition and facies.

Sample 19: $Na–Cl–SO_4–HCO_3$
Sample 24: $Na–SO_4–Cl$
Sample 29: $Na–Ca–HCO_3–SO_4–Cl$
Sample 32: $Na–HCO_3–Cl$

The geochemical facies of the samples show that there is a significant change in ionic composition and their association from the recharge to discharge and it is also different in different flow paths. Though Na seems to be the dominant cation in all the samples, the association of anions shows that in the flow path A1 they are dominantly associated with $SO_4–Cl$ and in flow path A2 they are dominantly associated with HCO_3. It is also noted that in the regions of discharge along the flow paths A1 and A2 the thermodynamic stability of composition seems to be closer than the chemical facies as witnessed in Piper plot (Fig. 11).

CONCLUSION

The hydrogeochemical evolution from the recharge to the discharge of the ground water is yet a challenging task to the hydrogeochemist, but still the attempt proves that, SI for carbonate minerals are negative, they are in the following order: Dolomite < Aragonite < Calcite. The SI of the silica is in the following order: $SI_{QTZ} > SI_{CHAL} > SI_{SiO_{2(a)}}$ (crystalline > cryptocrystalline > amorphous). The SI of secondary minerals in groundwater indicates, SI is of the following order: K-mica > Kaolinite > Ca-montmorillonite > Gibbsite > K-feldspar. The entire study area has been classified into initial, transitional and final stages of weathering based on SIy values. In the regions with initial stages of weathering SIy is positive and the negative values in the regions coincides with the regions of discharge or the final zones. The near zero values fall in the transitional zones. Phase mole transfer along the flow path A1 indicates that there is addition of phase moles noted in minerals like K-feldspar, marcasite, chlorite and kaolinite. The third model was calibrated as the field model out of the five models evolved. In flow path A2, removal of gibbsite and addition of K-feldspar, Ca-montmorillonite and marcasite was noted along its pathway. Decrease of ionic composition in flow path A1 and increase of it in flow path A2 is witnessed in the thermodynamic stability diagrams and Piper plot. The initial and final solutions in both the flow paths were correlated with the thermodynamic stability of groundwater and hydrogeochemical facies. It was found that the state of thermodynamic stability were almost similar at the discharge.
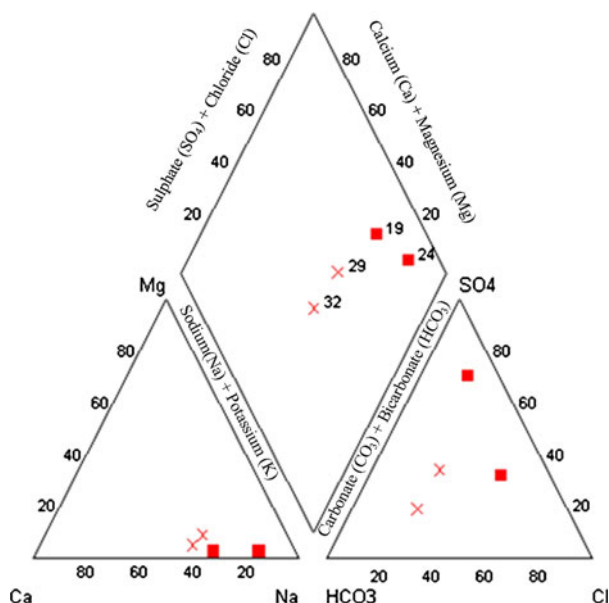
REFERENCES

Anandhan, P. (2005). *Hydrogeochemical studies in and around Neyveli mining region, Tamil Nadu, India.* Ph.D. Thesis, Department of Earth Sciences, Annamalai University, 189 pp.

APHA. (1995). *Standard methods for the examination of water and wastewater* (19th ed.). Washington, DC: APHA.

CGWB. (1992). *Report of the working group on the estimation of ground resources and irrigation potential of Periyar district, Tamil Nadu* (Unpublished Report).

Chidambaram, S. (2000). *Hydrogeochemical studies of groundwater in Periyar district, Tamil Nadu, India.* Unpublished Ph.D. Thesis, Department of Geology, Annamalai University, India.

Deutsch, W. J. (1997). *Ground water geochemistry: Fundamentals and application to contamination.* Boca Raton: Lewis Publishers.

Drever, I. J. (1988). *The geochemistry of natural waters* (2nd ed., 388 pp.). Englewood Cliffs, NJ: Prentice Hall.

Elangovan, K. (1997). *Hydrogeochemistry of groundwater forming heavy scales in water supply system of Salem district, Tamil Nadu* (334 pp.). Unpublished Ph.D. Thesis, Mysore University, Mysore.

Elangovan, K., Balasubramanian, A., Thirugnana Sambandam, R., Rengarajan, R., Satish, P. N., & Janardhan, A. S. (1999). Geochemical modeling of crystalline aquifers of Salem district, Tamil Nadu. *Indian J Geochem, 14,* 1–17.

Felmy, A. R., Bervin, D. C., & Jenne, E. A. (1984) *MINTEQ. A computer program for calculating aqueous geochemical equilibria.* US EPA 84-032, Athens GA.

Garrels, R. M., & Christ, C. L. (1965). *Solutions minerals and equilibria* (450 pp.). New York: Harper and Row.

Gibbs, R. J. (1970). Mechanisms controlling world's water chemistry. *Science, 170,* 1088–1090.

Gowrishanker, S., Meyyappan, M., & Radhakrishnan, M. (1980). Lignite deposits and groundwater development on Neyveli area. *Bullet. ONGC, 17,* 1–16.

Helgeson, H. C., Brown, T. H., Nigrini, A., & Jones, T. A. (1970). Calculation of mass transfer in geochemical processes involving aqueous solutions. *Geochimica et Cosmochimica Acta, 34,* 569–592.

Jenne, E. A. (1981). *Geochemical modeling: A review waste Rock interactions program.* Pacific North West laboratory Report 3574: VC70, 47 pp.

Konrad, B. K. (1983). *Introduction to geochemistry* (2nd ed.). New York: McGraw-Hill International Book Company.

Murphy, E. M., & Schramke, J. A. (1998). Estimation of microbial respiration rates in groundwater by geochemical modeling constrained with stable isotopes. *Geochimica et Cosmochimica Acta, 62*(21/22), 3395–3406.

Nordstrom, D. K., Plummer, L. N., Wigley, T. M. L., Wolery, T. J., Ball, J. W., Jenne, E. A., et al. (1979). A comparison of computerized chemical models for equilibrium calgllations in aqueous systems. In E. A. Jenne (Ed.), *Chemical modeling in aqueous systems* (pp. 857–892). Washington, DC: American Chemical Society, Symposium Series 93.

Parkhurst, DL., Thorstenson, DC., & Plummer, LN. (1990) PHREEQE—A computer program for geochemical calculation. USGS water resources investigations report 80-96, 195 pp.

Plummer, L. N., Busby, J. F., Lee, R. W., & Hanshaw, B. B. (1990). Geochemical modeling of the madison aquifer in parts of Montana, Wyoming and South Dakota. *Water Resources Research, 26,* 1981–2014.

Plummer, L. N., Jones, B. F., & Truesdell, A. H. (1976). *WATEQF—A fortran IV version of water, a computer program for calculating chemical equilibrium of natural waters.* US Geol Survey water resources investigations report 76, 1361 pp.

Plummer, L. N., Parkhurst, D. L., & Thorstenson, D. C. (1983). Development of reaction models for groundwater systems. *Geochimica et Cosmochimica Acta, 47,* 665–685.

Prasanna, M. V., Chidambaram, S., Srinivasamoorthy, K., Anandhan, P., & John Peter, A. (2006). A study on hydrogeochemistry along the ground water flow path in different litho units in Gadilam river basin, Tamil Nadu (India). *International Journal of Chemical Sciences, 2*(2), 157–172.

Ramanathan, A. L. (1992). *Geochemical studies in the Cauvery river basin.* Unpublished Ph.D. Thesis. Punjab University, Chandigarh, India.

Ramesh, R., & Anbu, M. (1996). *Chemical methods for environmental analysis: Water and sediment* (161 pp.) Madras: Macmillan India Ltd.

Runnels, D. D. (1978). American research in the geochemical modeling of groundwater. *Journal of the Geological Society of India, 29,* 135–144.

Sanford, W. E., & Konikow, L. F. (1989). Simulation of calcite dissolution and porosity change to in salt-water mixing zones in coastal aquifers. *Water Resources Research, 25,* 655–667.

Shannon, D. W., Morray, J. R., & Smith, P. R. (1977). *Use of a chemical equilibrium model computer code to analyze scale formation and corrosion in geothermal brines.* Proceedings in Symposium on Oil Field and Geothermal Chemistry Conference 770609, pp. 21–36.

Spostigo, G., & Mattigod, S. V. (1979). *GEOCHEM: A computer program for the calculation of chemical equilibria in soil solution and other natural water systems.* Riverside, CA: Department of Soil and Environmental Sciences, University of California.

Stumm, W., & Morgan, J. J. (1996). *Aquatic chemistry* (p. 1022 pp). New York: John Wiley and Sons Inc.

Tamata, S. R. (1990). Mineral-$CaCO_3$ saturation and stability of groundwater in Kamataka state—A preliminary study. *Bhu-Jal News 8–384,* 14–24.

Truesdell, A. H., & Jones, B. F. (1973). WATEQ: A computer program for calculating chemical equilibria of natural waters. *Journal of Research of the U.S. Geological Survey, 2*(2), 233–248.

Uma Maheswaran, T. (2007) *Hydrogeochemical modeling of in and around Devakottai region, Tamil Nadu.* M.Phil. Thesis, Department of Earth Sciences, Annamalai University.

Wolery, T. J. (1979). *Calculation of chemical equilibrium between aqueous solutions and minerals: The EQ3/EQ6 software package* (41 pp.). Livermore, University of California, Lawrence Livermore Laboratory (UCRL 52658).

Wolery, T. J. (1983). *EQ3NR: A computer program for geochemical aqueous specification—Solubility calculations* (191 pp.). Livermore, California: User's Guide and documentation, Lawrence Livermore National Lab UCRL-53414.

Zhu, C., & Anderson, C. (2002). *Environmental applications of geochemical modeling.* Cambridge: Cambridge University Press.